Relationship between Ice Water Path and Downward Longwave Radiation for Clouds Optically Thin in the Infrared: Observations and Model Calculations

TANEIL UTTAL

Wave Propagation Laboratory, NOAA Environmental Research Laboratories, Boulder, Colorado

SERGEY Y. MATROSOV

Cooperative Institute for Research in the Environmental Sciences, University of Colorado, Boulder, Colorado

JACK B. SNIDER AND ROBERT A. KROPFLI

Wave Propagation Laboratory, NOAA Environmental Research Laboratories, Boulder, Colorado

(Manuscript received 9 October 1992, in final form 9 July 1993)

ABSTRACT

A vertically pointing 3.2-cm radar is used to observe altostratus and cirrus clouds as they pass overhead. Radar reflectivities are used in combination with an empirical Z_i–IWC (ice water content) relationship developed by Sassen (1987) to parameterize IWC, which is then integrated to obtain estimates of ice water path (IWP). The observed dataset is segregated into all-ice and mixed-phase periods using measurements of integrated liquid water paths (LWP) detected by a collocated, dual-channel microwave radiometer. The IWP values for the all ice periods are compared to measurements of infrared (IR) downward fluxes measured by a collocated narrowband (9.95–11.43 μm) IR radiometer, which results in scattergrams representing the observed dependence of IR fluxes on IWP. A two-stream model is used to calculate the infrared fluxes expected from ice clouds with boundary conditions specified by the actual clouds, and similar curves relating IWP and infrared fluxes are obtained. The model and observational results suggest that IWP is one of the primary controls on infrared thermal fluxes for ice clouds.

1. Introduction

Cirrus and other thin nonprecipitating clouds have become the target of intensive research because of their seasonal and geographical prevalence and because of their ability to modify the atmospheric radiation budget (Liou 1986). Several experiments in the late 1980s and early 1990s designed to investigate the properties of these clouds include the Atmospheric Radiation Monitoring Experiment (ARM) (DOE 1990), the First ISCCP (International Satellite Cloud Climatology Project) Regional Experiments (FIRE I and II) (Starr 1987), and the Experimental Cloud Lidar Pilot Studies (ECLIPS I and II) (WMO 1988). In addition, the National Oceanic and Atmospheric Administration (NOAA) Wave Propagation Laboratory (WPL) conducted two Cloud Lidar and Radar Exploratory Tests, CLARET I in the fall of 1989 (Eberhard 1990), and CLARET II in the winter of 1990.

Corresponding author address: Dr. Taneil Uttal, R/E/WP6, 325 Broadway, Boulder, CO 80303.

The CLARET experiments were smaller in scope; however, they set a precedent of using a ground-based, multisensor approach, deploying collocated active and passive ground-based remote-sensing instruments to simultaneously gather information on cloud geometry, cloud microphysics, cloud phase, and cloud dynamics. This paper concentrates on comparing the relative effects of integrated liquid water path (LWP), integrated ice water path (IWP), cloud-base height, and cloud thickness on downward infrared (IR) radiative fluxes. In the past, atmospheric lidars have been more commonly used to study cirrus cloud characteristics; here we concentrate on data obtained by a 3-cm cloud-sensing radar. Companion papers from the CLARET experiments describe the derivation of ice water content (IWC), characteristic particle sizes, and mean particle concentrations using a combination of a ground-based radar and a narrowband IR radiometer (Matrosov et al. 1992); the calculation of profiles of effective particle radius from radar and lidar data (Intrieri et al. 1993); and studies of relationships between mean particle size characteristics and IR spectrometer measurements (Palmer et al. 1992).

2. Background

IWC (g m^{-3}) and its range integral IWP (g m^{-2}) are radiatively important parameters of thin clouds that are difficult to model or measure. These quantities are of considerable importance because IWP is critical for determining cloud absorption, optical depth (Platt and Harshvardhan 1988), albedo, and emissivity (Stephens 1980; Paltridge and Platt 1981). As are many cloud properties, IWC has been observed to be extremely variable, typically ranging over four orders of magnitude (10^{-4}–1.2 g m^{-3}; Dowling and Radke 1990) in cirrus clouds. However, because of the difficulties introduced by complex shape and size distributions of ice particles, as well as the need for a more complicated radiative transfer treatment, determining IWC and IWP is considerably more complicated than determining liquid water content (LWC) and LWP for warm clouds (Heymsfield and Platt 1984).

Methods for determining IWC or IWP fall into three categories. The first includes remote-sensing methods that use measurements from two sensors operating at two different wavelengths (Yeh and Liou 1983; Zhuravleva and Kostko 1986; Wu 1987; Matrosov et al. 1992). These methods typically involve passive radiation measurements and therefore provide information only on total IWP and not on the range-resolved structure of IWC in the cloud. A second approach has been to parameterize IWC based on thermodynamic models (Heymsfield and Donner 1990), and a third approach utilizes empirical relationships between IWC or IWP and a more easily observed quantity such as radiative attenuation (Novosel'tsev 1962), temperature (Heymsfield and Platt 1984; Kosarev and Mazin 1989), or radar reflectivities (Heymsfield 1977; Sassen 1987).

Because the CLARET I dataset provided continuous observations of cirrus and altostratus clouds with the NOAA/WPL 3-cm-wavelength cloud radar, this paper utilizes the empirical relationship developed by Sassen (1987), which is a reflectivity–ice water (Z_i–IWC) relationship tailored specifically for cirrus-type clouds.

3. Experiment

In 1989, NOAA/WPL conducted CLARET I near Boulder, Colorado, to observe cirrus clouds with vertically pointing remote sensors operating simultaneously at different wavelengths. These sensors were a microwave radar, an IR lidar, a visible lidar, a three-channel microwave radiometer, and an IR radiometer (PRT-5) with a narrowband filter. A contingent of standard surface radiation sensors included a pyranometer, a pyrgeometer, and a pyrheliometer operated by NOAA's Climate Modeling and Diagnostics Laboratory (CMDL); satellite measurements were also collected. The nearest rawinsonde site was the Denver National Weather Service office, which has a normal 12-h release schedule. The operating frequencies and parameters of the instruments used in this study are summarized in Table 1.

A primary objective of the experiment was to test the ability of the NOAA/WPL sensors to observe cirrus cloud characteristics. This included expanding and improving techniques for observing cirrus cloud properties using remote sensors singly and in combination. A notable part of this exercise was the use of long dwells (see discussion below) to improve the signal-to-noise ratios for the radar.

The field campaign concentrated on the most simple and direct way to observe such clouds, that is, pointing all the sensors vertically except for brief periods when the radar and lidar would do quick "surveillance" RHIs (scanning from horizon to horizon at a fixed azimuth).

Cirrus unobstructed by lower clouds was observed over the site for short periods on 7 of 29 days during the experiment. A total of 22 h of data was collected in an intensive operating mode when the cirrus could be detected by the radar. This does not include three additional days when cirrus existed above low-level overcast and accompanying drizzle. In general, the continental United States is covered by cirrus 25%–30% of the time, with only slight seasonal dependence (Dowling and Radke 1990) and the incidence of observable cirrus during the experiment was lower than expected. This was due partially to a record-setting wet September in 1989 with an abundance of low-level precipitating clouds. Such clouds interfere with upper-level cloud measurements by lidars, which would attenuate, and by the radiometers that make path-integrated measurements and would be unable to separate the effects of different cloud layers. Also, the 3 cm is not an optimum wavelength for cirrus detection, which also contributed to further downsize a relatively small data sample.

4. Data reduction considerations

a. Beam averaging

Radar signal processing involves averaging many echo samples to achieve the desired signal-to-noise ratio

TABLE 1. Operating frequencies of the CLARET I instruments used in this analysis.

Instrument	Frequency (GHz)	Parameters
Microwave radar	9.4	reflectivity velocity depolarization
Three-channel radiometer	20.6 31.6 90.0	integrated liquid integrated vapor
IR radiometer	2.6×10^4–3.0×10^4	IR radiance

and to reduce the variance of Doppler velocity. Because of the relatively weak radar signal from cirrus clouds, it is especially important to average as many radar pulses as are compatible with a cloud's natural variability to increase signal strength without losing information on small-scale features. In previous boundary-layer and convective storm studies performed with this 3-cm radar, it has been typical to average less than 200 pulses, and the radar processor was limited to averaging no more than 512 pulses. Nevertheless, the system has a designed flexibility (Pasqualucci et al. 1983) that allows for unlimited averaging after the data are collected.

For cirrus clouds, we determined that averaging over several seconds was a good compromise between considerations of signal-to-noise ratio and cloud variability; the CLARET I data were therefore averaged over 4 s or 5120 radar pulses whenever the radar was pointing vertically. The improved cirrus detection resulting from increasing the radar dwell was demonstrated by Uttal et al. (1990).

b. *Infrared radiometer calibration*

For accurate, ground-based IR remote sensing of atmospheric brightness temperatures, IR radiometer output voltages must be calibrated with an appropriate thermal source in the laboratory. WPL uses a blackbody simulator composed of a conical copper cavity painted black and submersed in a bath of alcohol mixed with dry ice. The PRT-5 was calibrated to −68°C for the CLARET I project. Significant errors can result, especially at cold temperatures (< −60°C) where blackbody simulation is increasingly difficult. Additional errors can result from temperature fluctuations of the radiometer cavity during calibration and inadequate accuracy in the measurement of radiometer and thermistor voltages. Therefore, even for a properly calibrated PRT-5, measured temperature errors of ±1.0°C can result between +20° and −30°C, ±2°–3°C between −30° and −60°C, and greater than 6°C below −60°C. The observed atmospheric brightness temperatures were as low as −75°C, and errors were estimated below −68°C by extrapolation of the calibration curve. Detailed PRT-5 calibration techniques are discussed by Shaw (1991).

c. *Calculation of IWC from radar reflectivity*

Sassen (1987) developed an equation relating radar reflectivities to IWC using three datasets collected on low-level polar ice clouds by Sato et al. (1981) and Kikuchi et al. (1982). IWC and radar reflectivities were calculated from the size spectra and concentrations of the particles precipitating to the ground. The resulting Z_i–IWC relationship,

$$\text{IWC (g m}^{-3}) = 0.037 Z_i^{0.696} \text{ (mm}^6 \text{ m}^{-3}), \quad (1)$$

was considered to be applicable to cirrus clouds because of the microphysical similarities between the two types of clouds. Since radar reflectivities are usually calculated using the dielectric constant for water, we corrected our equivalent reflectivity factors to utilize the dielectric constant for ice (a factor of 5.3), as is appropriate for the observation of predominantly ice clouds. Radar reflectivities adjusted in this manner are referred to with the notation Z_i. Heymsfield (1977) also developed a Z_i–IWC relationship for ice clouds based on data collected by aircraft and radar, and that relationship is compared to Sassen's in Fig. 1. The two relationships show good agreement for radar reflectivities between −25 and −5 dBZ, which is within the range of observed values for this study.

d. *Theoretical calculations of IWP–brightness temperature relationships*

Matrosov et al. (1992) has developed a method that allows the theoretical calculation of downwelling brightness temperatures of the cloud thermal radiation as a function of IWP for horizontally and vertically homogenous clouds. The method is based on a quadrature two-stream radiative transfer model (Toon et al. 1989), and cirrus particles are treated as solid ice spheres.

Since the two-stream model estimated brightness temperatures for comparison with the PRT-5, calculations were made in the IR transparency "window" from 9.95 to 11.43 μm, which corresponded to the bandwidth of the PRT-5. The two-stream model is particularly suited to this application since the scattering contribution in the radiative transfer is mostly localized in the forward direction, and we are interested in the downwelling radiation fields that would be measured by the zenith pointing PRT-5.

The spherical particle assumption is justified by the fact that ice absorbs radiation at these frequencies very

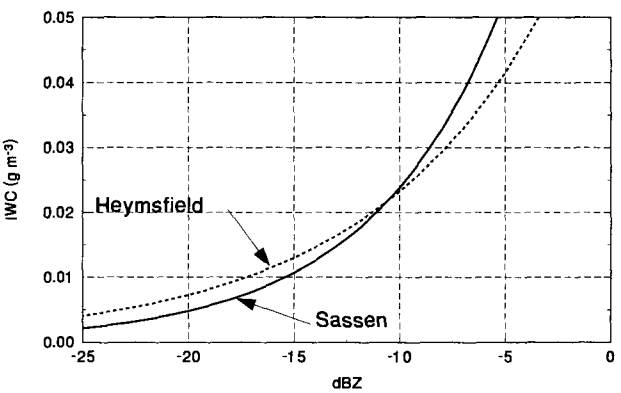

FIG. 1. Ice water content–radar reflectivity relationships derived by Sassen (1987) and Heymsfield (1977). Normal water equivalent radar reflectivities are on the x axis.

strongly, which allows simplification of the radiation transfer treatment. In addition, modeling absorbing particles that are large compared with incident wavelength as equivalent cross-sectional-area spheres is appropriate since we are primarily interested in absorption and forward scattering (Bohren and Singham 1991). Mie theory was used to calculate parameters needed for the radiative transfer calculations, for example, the extinction coefficient, the single scattering albedo, and the asymmetry factor. Particle size distribution was modeled by a gamma function of the first order with two free parameters: particle concentration and median particle diameter. Different IWP values were obtained by changing the concentrations (3–1000 L^{-1}) for different fixed values of median particle diameter ranging between 40 and 220 μm.

Cloud geometrical thickness was obtained from radar measurements of cloud boundaries. PRT-5 measurements made during a brief cloud-free period provided information for calculating the effective temperature and transmittance of the intervening atmosphere. Cloud temperature in the calculations was assumed to be constant and equal to the midcloud temperature measured by a rawinsode launch.

The inaccuracies in PRT-5 measurements described in section 4b primarily affect the measurements of background clear-sky radiation. Sensitivity studies indicate that the brightness temperature calculations for IWP > 20 g m^{-2} are relatively insensitive to several degree errors in the clear-sky brightness temperatures because of the large differences between cloud thermal radiation and the background sky radiation.

5. Results

a. 1900–2130 UTC 4 October

On 4 October 1989, between 1900 and 2130 (all times UTC), we observed an altostratus cloud characterized by stable cloud-base height and thicknesses but with significant variations in cloud radiative properties and radar reflectivities. The observed cloud resulted from a low pressure system over the western states feeding moisture from Tropical Depression Raymond to create precipitation and cloudiness over the experimental area. Earlier in the day, cirrus clouds over Boulder were between 6.5 and 9 km above ground level (AGL), but by 1900 they had lowered to 4–6 km as convective forcing from the tropical storm decreased.

Figure 2 shows time series plots of cloud boundaries from the radar, integrated vapor from the microwave radiometer, integrated liquid from the microwave radiometer, IWP from radar reflectivities using the Sassen Z_i–IWC relationship, and sky brightness temperatures from the IR radiometer. Rawinsonde temperatures are indicated on the right-hand y axis of Fig. 2a. Data gaps occurred in the radar data when the radar was performing other kinds of nonzenith-pointing scans. During the first of these data gaps, between 1930 and 1955 UTC, the PRT-5 data indicate that the cloud briefly dissipated over the remote-sensing site, which allowed an unobstructed clear-sky measurement of about −75°C. This is somewhat warmer than usual for Colorado in October; however, the lower temperature could be accounted for by the higher than average vapor contents of 1.4–1.6 cm (the average for this season would normally be about 1.0–1.2 cm). Brightness temperatures of the cloud thermal emission varied between −20° and −65°C. Over the 2.5-h period, cloud boundaries were relatively stable; tops were between 6 and 7 km AGL, and bases started at 4 km and slowly lowered to 3 km. The cloud thickness varied from 1.2 km around 2000 to 3.1 km at 2125 UTC. Liquid water amounts were quite variable in this cloud, varying from 0 to 0.16 mm. IWP parameterized by radar reflectivity was also variable ranging from 10 to 170 g m^{-2}.

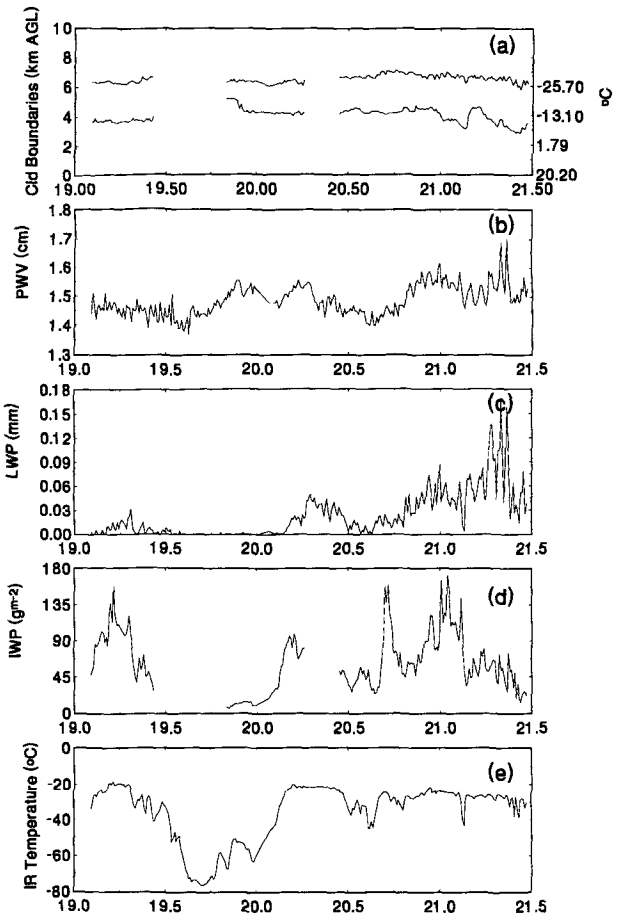

FIG. 2. Time series for 4 October 1989: (a) cloud boundaries from radar, (b) precipitable water vapor from dual-channel microwave radiometer, (c) liquid water path from dual-channel microwave radiometer, (d) ice water path from radar reflectivity, and (e) IR brightness temperature from IR radiometer. Rawinsonde temperatures are indicated on the right-hand y axis.

Figure 3 shows scatterplots of IR (PRT-5) brightness temperatures versus cloud thickness, cloud-base height, and IWP. Although there is in general the expected trend between brightness temperature and cloud thickness (warmer temperatures as thickness increases), as well as between brightness temperature and cloud-base height (temperature decreases as cloud-base height increases), there is wide scatter in this data. A more consistent relationship exists between cloud brightness temperature and the IWP parameter calculated from radar reflectivities. Figure 4 shows that

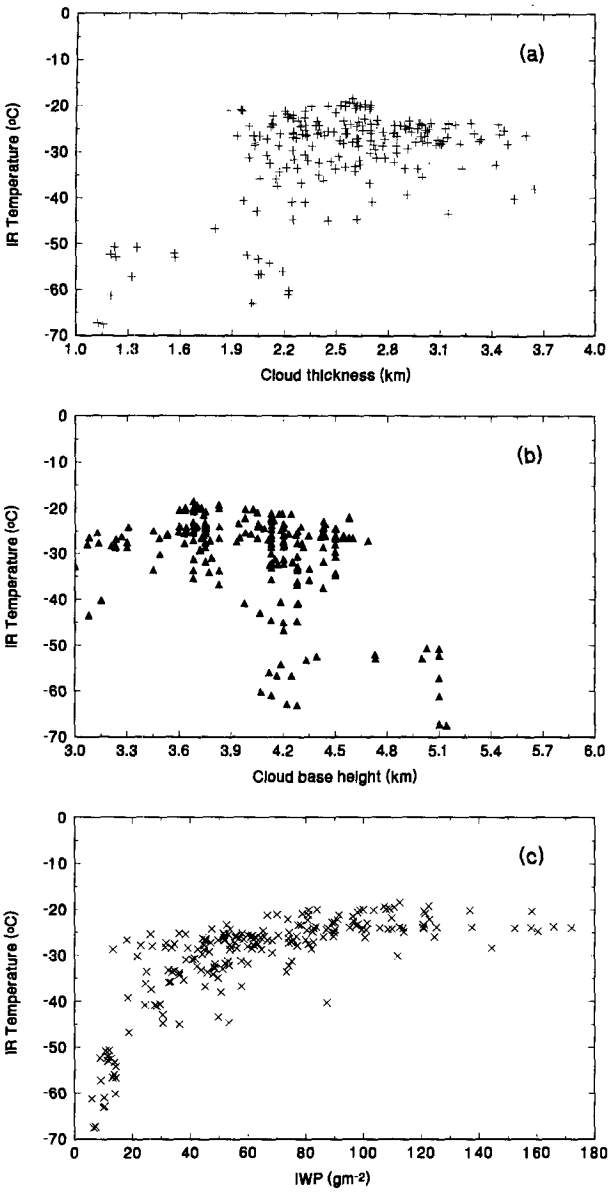

FIG. 3. Scatterplots for 4 October 1989: (a) cloud thickness vs IR brightness temperature, (b) cloud-base height vs IR brightness temperature, and (c) IWP vs IR brightness temperature.

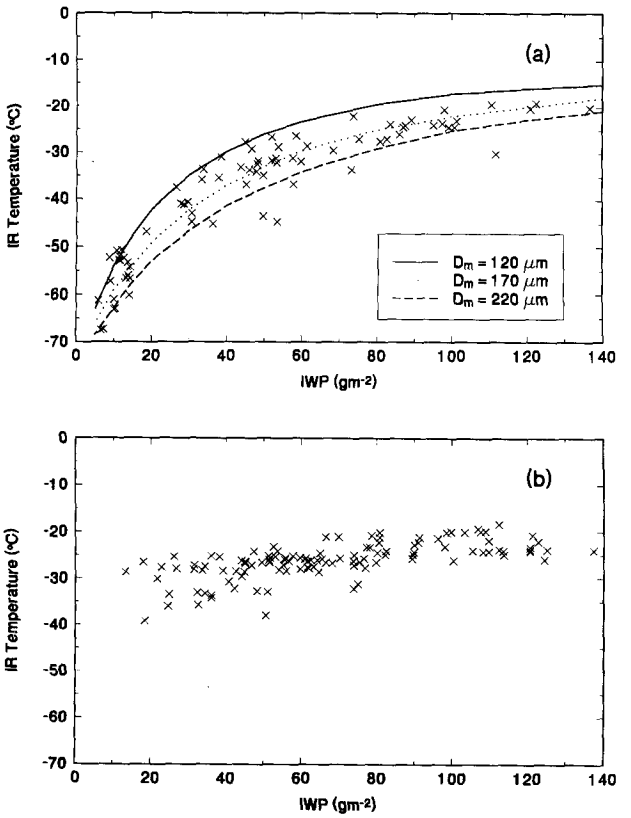

FIG. 4. Scatterplots for 4 October 1989, where IWP vs IR brightness temperature is partitioned: (a) LWP < 0.01 mm, and (b) LWP > 0.01 mm. Panel (a) also shows theoretical curves of IWP vs IR brightness temperature for mean particle diameters of 120, 170, and 200 μm.

additional insight can be gathered by partitioning the data based on LWP. Figure 4a shows the data points where corresponding measurements of LWP greater than 0.01 mm were deleted; the remaining points show the relationship between cloud brightness temperature and IWP when the cloud was strictly an ice cloud, and no complicating radiative effects were introduced by a mixed ice–liquid phase. Figure 4a also has curves from the theoretical calculations of cloud brightness temperature versus IR fluxes for three values of median particle diameter, 120, 170, and 220 μm. This result combined with the observations suggests that the particles in this cloud had median diameters between 120 and 220 μm. The data points that were deleted on the basis of the criterion of LWP greater than 0.01 mm (Fig. 4b) demonstrate expected behavior in that they occur at warmer cloud temperatures, between −40° and −20°C, and mostly warmer than −30°C. Comparison of the PRT −5 brightness temperatures with cloud-base temperature measured by the rawinsonde suggests that the liquid water caused the cloud to radiate at the midcloud atmospheric temperatures.

b. 1428–1615 UTC 28 September

A low pressure center off the coast of California was blocked by a persistent high pressure ridge over the southwestern United States that had resulted in a prolonged period of sunny dry weather during the last week of September. To the north, a trough axis moved slowly southeastward and combined with a brief pulse of moisture on 27 and 28 September, resulting in light showers and light, intermittent, high-level clouds over Colorado. These clouds were observed over the remote sensing site as they dissipated on the morning of 28 September. The clouds were confined between 6 and 9 km AGL.

Figure 5 shows time series data for 28 September that correspond to those of Fig. 2 for 4 October. The time periods when no cloud is indicated is a combination of periods when the radar was not scanning vertically, as well as a brief period between 1509 and 1516 UTC when the 3-cm radar was unable to detect the cloud. The presence of cloud was indicated by both lidar measurements and IR brightness temperatures higher than those of clear sky. Cloud-base heights varied rapidly between 6.1 and 7.9 km, and cloud-top heights varied between 6.8 and 8.3 km. Water vapor amounts were again high (1.7 cm) for this time of year over Colorado, partially accounting for high clear-sky brightness temperatures of about −70°C. This cloud had no detectable liquid and therefore was considered to be an all-ice cloud. IWP did not exceed 70 g m^{-2}, and the warmest brightness temperatures observed were −30°C, with mean temperatures of about −50°C. Figure 6 shows scatterplots of brightness temperatures versus cloud thickness, cloud-base height, and IWP. In this experimental period, there was a somewhat stronger relationship between cloud thickness and brightness temperatures, which indicates that the cloud may have been more homogenous than the 4 October cloud. As in the 4 October cloud, cloud-base height and cloud brightness temperatures have no obvious relationship in the 28 September cloud.

Scatterplots of cloud brightness temperature and IWP again show a significant relationship that agrees well with theory (Fig. 7). Calculated curves of cloud brightness temperature versus IWP are shown for mean particle diameters of 40, 120, and 200 μm. Based on matching observed data to theoretical curves, it would appear that the colder portions of the cloud (−70° to −40°C) had particles with mean diameters near 30–45 μm and the warmer portions of the cloud had particles with mean diameters closer to 120 μm. This dependence of diameter on temperature is consistent with microphysical arguments presented by Heymsfield and Platt (1984).

6. Discussion of results

Results for the two cases described in the previous section and for two other shorter periods earlier on 4 October are summarized in Table 2. The two shorter periods between 0200 and 0220 UTC and 0230 and 0245 UTC were defined as two separate cases based on a consistent 1-km difference in cloud-base height. The table summarizes cloud height, brightness temperature, IWP, LWP, and median particle diameter based on matching the observed data to the theoretical curves. Two particularly interesting features are apparent. First, cloud IWP and LWP (millimeters converted to grams per square meter for comparison to IWP) exist in comparable amounts for all three time periods examined on 4 October, showing that even at high, cold altitudes in the atmosphere, the liquid phase can be a significant component of cloud mass (Sassen et al. 1989). This is in contrast to the case on 28 September, which is more representative of the classic cirrus cloud, composed strictly of ice and no detectable liquid. Second, values of median particle diameter show

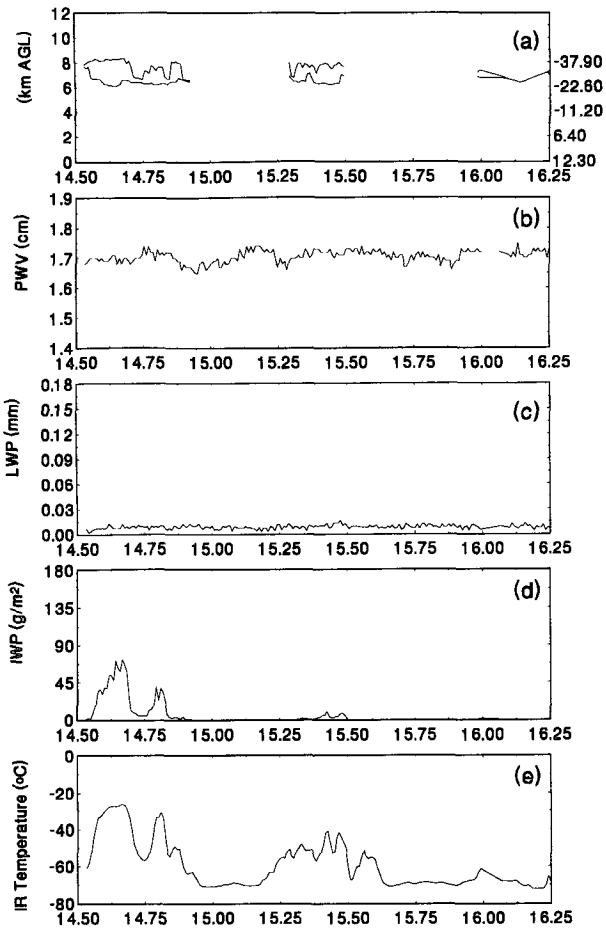

FIG. 5. Time series for 28 September 1989: (a) cloud boundaries from radar, (b) precipitable water vapor from dual-channel microwave radiometer, (c) liquid water path from dual-channel microwave radiometer, (d) ice water path from radar reflectivity, and (e) IR brightness temperature from IR radiometer. Rawinsonde temperatures are indicated on the right-hand y axis.

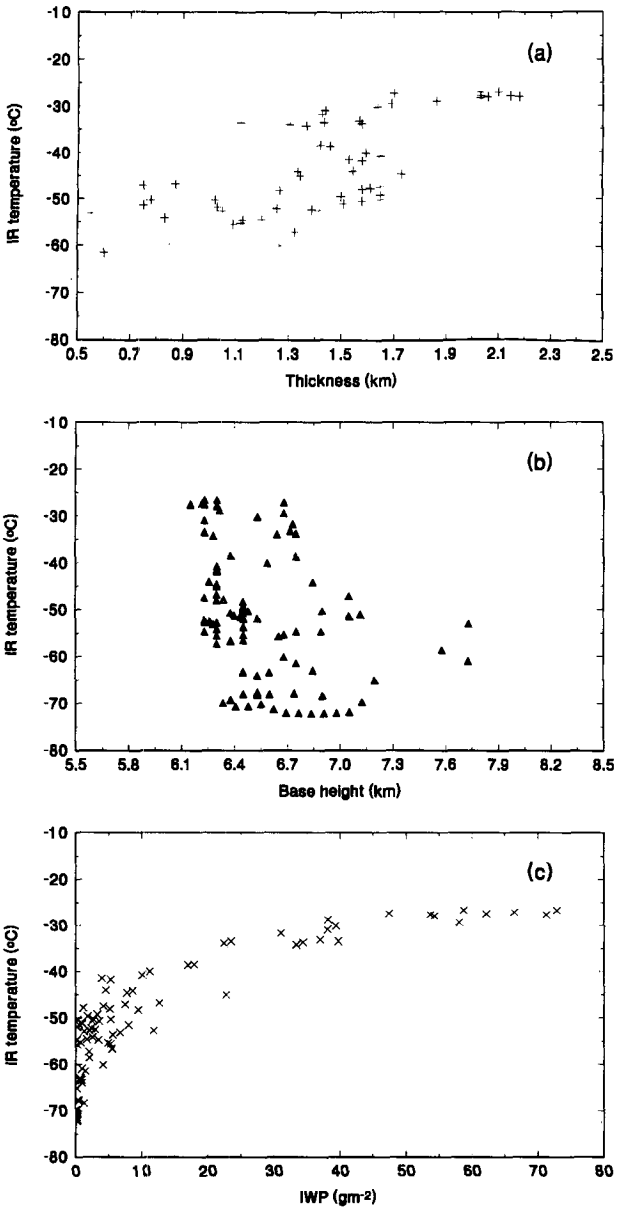

FIG. 6. Scatterplot for 28 September 1989: (a) cloud thickness vs IR brightness temperature, (b) cloud-base height vs IR brightness temperature, and (c) IWP vs IR brightness temperature.

a trend of particle size decreasing with altitude, ranging from about 150 μm in the cloud at 5 km AGL to about 10 μm in the cloud centered at 8 km AGL.

The method described by Matrosov et al. (1992) also allows estimates of vertically averaged particle sizes and concentrations from measurements of IR brightness temperature and radar reflectivities. This size and concentration information was used to estimate IWP denoted as (IWP_{model}). The technique utilizes the fact that both radar reflectivity and IR radiation vary as a function of particle size and concentration, allowing the solution of two equations for two unknowns. These values were compared to the values of IWP obtained using Sassen's empirical relationship (1), denoted as $IWP_{empirical}$. Figures 8a and 8b compare $IWP_{empirical}$ and IWP_{model} for 1905–2130 UTC 4 October, and 1428–1615 UTC 28 September, respectively. Only experimental points corresponding to the pure ice-phase cloud are shown. The regression equations are

$$IWP_{empirical} = 1.20(IWP_{model}) - 5.4 \quad \text{(4 October)} \quad (2)$$

$$IWP_{empirical} = 0.62(IWP_{model}) - 3.5 \quad \text{(28 September)}. \quad (3)$$

The agreement between Sassen's empirical method and Matrosov's inverse solution technique is surprisingly good for the 4 October case. The 28 September case shows more scatter and less agreement between the absolute values derived by the two methods despite the fact that this case is closer to a "classical" cirrus case. However, given that IWP varies by several orders of magnitude in cirrus clouds, values of 1.2 and 0.62 for the slopes of the linear regression fits are much better than expected especially since (1) represents an average empirical relationship that does not account for the variation of cirrus particles size, concentrations, and habits in individual cirrus clouds.

7. Concluding remarks

These results demonstrate that a radar can be an important tool in the observation of optically thin clouds. Radar reflectivities were interpreted as a measure of cloud IWC through an empirical Z_i–IMC relationship developed by Sassen (1987) and were used to calculate IWP. Among the cloud properties mea-

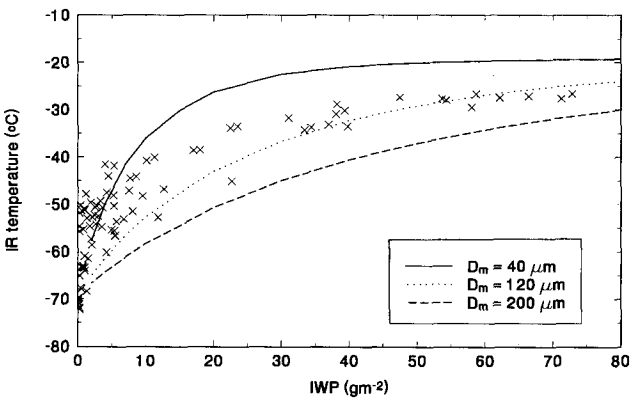

FIG. 7. Scatterplot for 28 September 1989: IWP vs IR brightness temperature with theoretical curves of IWP vs IR brightness temperature for mean particle diameters of 40, 120, and 200 μm.

TABLE 2. Summary of cloud characteristics.

	1430–1615 UTC 28 September	1900–2130 UTC 4 October	0200–0220 UTC 4 October	0230–0245 UTC 4 October
Height (km)	6.2–8.0	4.0–6.5	7.0–9.0	6.0–8.5
IR brightness temperature (°C)	−70° to −30°	−75° to −20°	−60° to −30°	−50° to −30°
LWP (g m^{-2})	<10	10–140	10–20	10–20
IWP (g m^{-2})	0–60	0–160	0–20	0–30
D_m	30–100	170	10	30

sured, IWP appears to be the primary control on downward IR flux properties of the cloud, exceeding the effects of cloud thickness and cloud-base height. This result clearly indicates that the location of cloud boundaries will not be sufficient to determine cloud radiative properties for optically thin clouds. The dependence of cloud longwave fluxes on cloud particle sizes, while significant, appears to be a secondary effect for situations where there is a large dynamic range of IWP values.

This result has been also suggested by Ebert and Curry (1992), who examined the relative effect of varying particle size versus IWP on the shortwave reflectivity and the longwave radiation. Their modeling results indicate that reflectivity, transmissivity, and emissivity all vary significantly as a function of IWP and characteristic ice-particle sizes. However, changes in ice particle sizes were more dominant in altering the shortwave reflectivity, whereas changes in total IWP were the primary control in determining the values of longwave radiation.

It is encouraging that the functional form of the observed data matches well with that predicted with simple theoretical calculations based on a two-stream model and spherical particle assumptions. This theoretical relationship has been demonstrated by others (Smith et al. 1990; Ebert and Curry 1992), and this paper clearly demonstrates that the observed data show the same trends and values expected from theory. It is also significant that over a relatively short time period the observed clouds showed a wide variation in IWP values and resulting values of downward IR fluxes, despite the fact that in some cases cloud boundaries were quite stable.

Empirical Z_i–IWC relationships can only be expected to be successful when the relationships are applied to clouds that are microphysically similar to the cloud from which the relationship was derived. In theory, techniques such as those described by Matrosov et al. (1992), which incorporate measurements from two sensors to obtain a closed set of two equations with two unknowns, incorporate more physics and are more sound. This latter technique, however, uses longwave flux measurements as an input, which is a parameter that would sometimes be useful to predict from cloud characteristics, saving the real measurements for verification.

Given the difficulties of measuring and modeling radiatively important microphysical properties of clouds such as particle size and concentration, it is promising that a bulk parameter like IWP, which depends on those two quantities, may be sufficient to specify the flux properties of clouds for climate studies. Empirical equations are easier to use for estimating cirrus cloud IWP, and it has been shown in this paper that in some cases the results are very close to those obtained using quadrature two-stream techniques. This conclusion mirrors that put forth by Paltridge and Platt (1981). They concluded their remarks with the concern as to whether such a parameterization would be adequate. This work, in combination with the work of others, suggests that such IWP parameterizations could indeed be adequate for modeling longwave cloud fluxes.

Further work on this topic will include application of Z_i–IWC relationships to other optically thin clouds, as well as verification with in situ data from aircraft, cloud sondes, and other remote sensing techniques. We also anticipate the development of techniques using the IR radiometer to specifically tailor the coefficient and the exponent in the IWC–aZ_i^b relationship to more accurately reflect conditions in specific clouds.

Datasets that have since been collected with the NOAA Ka-band radar, which operates at 8 mm, have demonstrated the superior performance of this shorter wavelength radar for observing nonprecipitating ice clouds (Kropfli et al. 1990). The techniques described in this paper will be applied to datasets collected with that radar during the First ISCCP Regional Experiment (FIRE II) conducted in Coffeyville, Kansas, during winter 1991 and also during the Atlantic Stratocumulus Transition Experiment (ASTEX) conducted in the Azores during the summer of 1992.

Acknowledgments. The authors would like to thank the many people involved with collecting and processing the data for the CLARET project. These include K. Clark, J. Gibson, B. Bartram, E. Ash, M. Jacobson, L. Church, B. Martner, and B. Orr. W. Eberhard coordinated the CLARET project and provided many

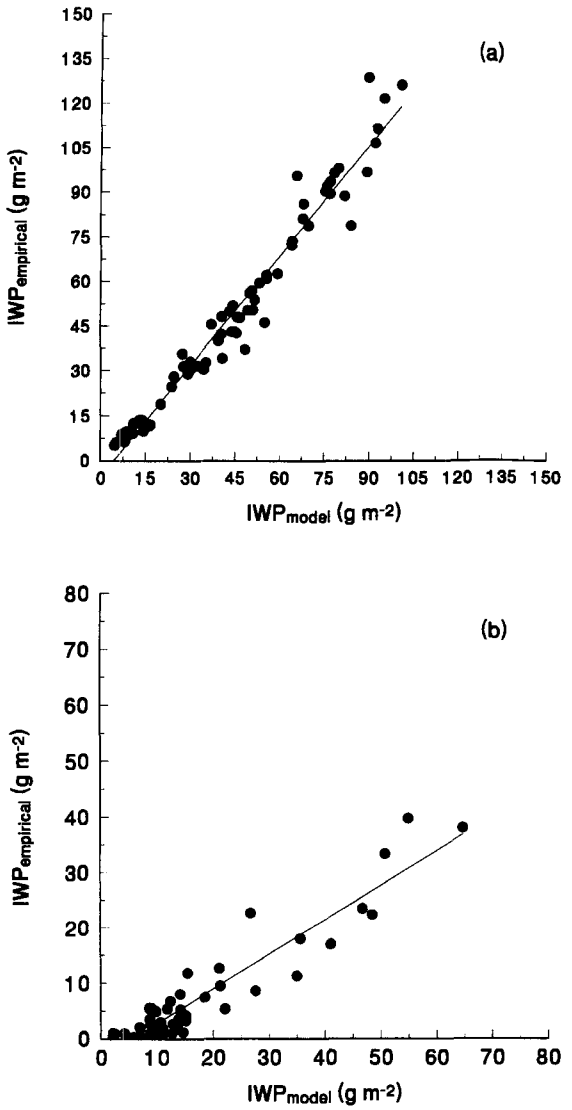

FIG. 8. Scatterplot comparing IWP calculations using the empirical method developed by Sassen (1987), IWP_s and the theoretical method developed by Matrosov (1992), IWP_m: (a) 4 October 1989 and (b) 28 September 1989.

useful discussions. Partial funding for CLARET I was provided by DOE/ARM Earth Science and Applications Division under Grant DE-AI06-91RL12089 and partially by NASA 4020-CL-387.

REFERENCES

Bohren, C. F., and S. B. Singham, 1991: Backscattering by nonspherical particles: A review of methods and suggested new approaches. *J. Geophys. Res.*, **96,** 5269–5277.

DOE, 1990: Atmospheric radiation measurement program plan. DOE/ER-0441, U.S. Dept. of Energy, Atmospheric and Climate Research Division, 116 pp. [NTIS DE90-102755.]

Dowling, D. R., and L. F. Radke, 1990: A summary of the physical properties of cirrus clouds. *J. Appl. Meteor.*, **29,** 970–978.

Eberhard, W., T. Uttal, J. M. Intrieri, and R. J. Willis, 1990: Cloud parameters from IR lidar and other instruments: CLARET design and preliminary results. Preprints, *Seventh Conf. on Atmos. Radiation,* San Francisco, CA., Amer. Meteor. Soc. 343–348.

Ebert, E. E., and J. A. Curry, 1992: A parameterization of ice cloud optical properties for climate models. *J. Geophys. Res.*, **97,** 3831–3836.

Heymsfield, A. J., 1977: Precipitation development in stratiform ice clouds: A microphysical and dynamical study. *J. Atmos. Sci.*, **34,** 367–381.

——, and L. J. Donner, 1990: A scheme for parameterizing ice-cloud water content in general circulation models. *J. Atmos. Sci.*, **47,** 1865–1877.

——, and C. M. R. Platt, 1984: A parameterization of the particle size spectrum of ice clouds in terms of the ambient temperature and ice water content. *J. Atmos. Sci.*, **41,** 846–855.

Intrieri, J. M., G. L. Stephens, W. L. Eberhard, and T. Uttal, 1993: A method for determining cirrus cloud particle sizes using a lidar and radar backscatter technique. *J. Appl. Meteor.*, **32,** 1074–1082.

Kikuchi, K., S. Tsuboya, N. Sato, and Y. Asuma, 1982: Observation of wintertime clouds and precipitation. Part 2: Characteristic properties of precipitation particles. *J. Meteor. Soc. Japan,* **60,** 1215–1225.

Kosarev, A. L., and I. P. Mazin, 1989: Empirical model of physical structure for the upper-level clouds of middle latitudes. *Radiation Properties of Cirrus Clouds,* Nauka, 29–53.

Kropfli, R. A., B. W. Bartram, and S. Y. Matrosov, 1990: The upgraded WPL dual-polarization 8.6 mm Doppler radar for microphysical and climate research. Preprints, *Conf. on Cloud Physics,* San Francisco, CA, Amer. Meteor. Soc., 341–345.

Loiu, K. N., 1986: Influence of cirrus clouds on weather and climate processes: A global perspective. *Mon. Wea. Rev.*, **114,** 1167–1199.

Matrosov, S. Y., T. Uttal, J. B. Snider, and R. A. Kropfli, 1992: Estimation of ice cloud parameters from ground-based infrared radiometer and radar measurements. *J. Geophys. Res.*, **97,** 11 567–11 574.

Novosel'tsev, Ye. P., 1962: On the water content of upper-level clouds. *Meteor. Gidrol.*, **8,** 31–32.

Palmer, A. J., S. Y. Matrosov, B. E. Martner, T. Uttal, D. K. Lynch, M. A. Chatelain, J. A. Hackwell, and R. W. Russell, 1992: Combined infrared emission spectra and radar reflectivity studies of cirrus clouds. *IEEE J. Geosci. Remote Sens.*, submitted.

Paltridge, G. W., and C. M. R. Platt, 1981: Aircraft measurements of solar and infrared radiation and the microphysics of cirrus cloud. *Quart. J. Roy. Meteor. Soc.*, **107,** 367–380.

Pasqualucci, F., B. W. Bartram, R. A. Kropfli, and W. R. Moninger, 1983: A millimeter-wavelength dual-polarization Doppler radar for cloud and precipitation studies. *J. Appl. Meteor.*, **22,** 758–765.

Platt, C. M. R., and Harshvardhan, 1988: Temperature dependence of cirrus extinction: Implications for climate feedback. *J. Geophys. Res.*, **93,** 11 051–11 058.

Sassen, K., 1987: Ice cloud content from radar reflectivity. *J. Atmos. Sci.*, **26,** 1050–1053.

Sato, N. K., K. Kikuchi, S. C. Barnard, and A. W. Hogan, 1981: Some characteristic properties of ice crystal precipitation in summer season at South Pole Station, Antarctica. *J. Meteor. Soc. Japan,* **59,** 772–780.

Shaw, J. A., 1991: Calibration of infrared radiometers for cloud-base temperature remote sensing: Technique and error analysis. NOAA Tech. Memo. ERL WPL-207, NOAA Environmental Research Laboratories. [NTIS PB92-102755.]

Smith, W. L. Jr., P. R. Hein, and S. K. Cox, 1990: The 27–28 October 1986 FIRE IFO cirrus case study: In situ observations of radiation

and dynamic properties of a cirrus cloud layer. *Mon. Wea. Rev.*, **118,** 2389–2401.

Starr, D. O'C., 1987: A cirrus cloud experiment: Intensive field observations planned for FIRE. *Bull. Amer. Meteor. Soc.*, **67,** 119–124.

Stephens, G. L., 1980: Radiative properties of cirrus clouds in the infrared region. *J. Atmos. Sci.*, **37,** 435–446.

Toon, O. B., C. P. Mckay, T. P. Ackerman, and K. Santhanam, 1989: Rapid calculation of radiative heating rates and photodissociation rates in inhomogenous multiple scattering atmospheres. *J. Geophys. Res.*, **94,** 16 287–16 301.

Uttal, T., R. A. Kropfli, W. L. Eberhard, and J. M. Intrieri, 1990: Observations of mid-latitude, continental cirrus clouds using a 3.2 cm radar: Comparisons with 10.6 micron lidar observations, Preprints, *Seventh Conf. on Atmospheric Radiation,* San Francisco, CA, Amer. Meteor. Soc., 349–353.

WMO, 1988: An experimental cloud lidar pilot study (ECLIPS). WMO/TD-No. 251, World Meteorological Organization, Report of the WCRP/CSIRO Workshop on Cloud Base Measurement, 34 pp.

Wu, Man-Li C., 1987: Determination of cloud ice water content and geometrical thickness using microwave and infrared radiometric measurements. *J. Climate Appl. Meteor.*, **26,** 878–884.

Yeh, H. Y., and K. L. Liou, 1983: Remote sensing of cloud parameters from a combination of infrared and microwave channels. *J. Climate Appl. Meteor.*, **22,** 201–213.

Zhuravleva, V. A., and O. K. Kostko, 1986: Lidar–radiometric method for determining the ice water content of cirrus clouds. *Izv., Atmos. Ocean. Phys.*, **22,** 32–38.